

Supporting Information:

Hydrophobic solvation increases thermal conductivity of water.

Carlos López-Bueno*[a], Manuel Suárez-Rodríguez, [a], Alfredo Amigo [c], and Francisco Rivadulla*[a,b]

[a] CIQUS, Centro de Investigación en Química Biolóxica e Materiais Moleculares, Universidade de Santiago de Compostela, 15782-Santiago de Compostela, Spain.

[b] Departamento de Química-Física, Universidade de Santiago de Compostela, 15782-Santiago de Compostela, Spain.

[c] Departamento de Física Aplicada, Facultad de Física, Universidade de Santiago de Compostela, 15782-Santiago de Compostela, Spain.

* E-mail: carloslopez.bueno@usc.es ; f.rivadulla@usc.es

1.- THERMAL CONDUCTIVITY AND DIFFUSIVITY

We measure the thermal conductivity and thermal diffusivity of ethanol, 2-propanol and 1-propanol. The results are shown in Figure S1, including the heat capacity and density used for thermal diffusivity calculations. It is observed that the maximum in thermal conductivity and diffusivity is displaced to lower concentrations for isopropanol, and disappears completely in 1-propanol, showing the importance of the size and shape of the hydrophobic chains.

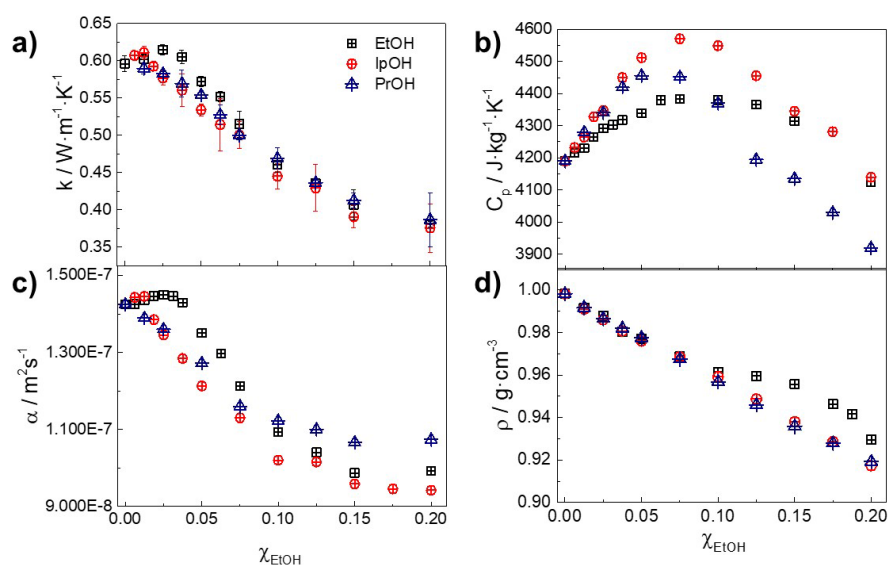


Figure S1. Thermal conductivity (a), heat capacity (b), thermal diffusivity (c) and density (d) for ethanol and 1- and 2-propanol at different concentrations. Note also de anomaly in the density of ethanol between $x=0.1$ - 0.2 .

The appearance of ice-like structures in liquid water under cooling produces several well-known anomalies, like a density maximum, a minimum in the adiabatic compressibility¹ or a $d\kappa/dT > 0$.² Consequently, we also analyzed the temperature dependence of κ for the different regimes, as we expect a transition from the characteristic positive slope in water to the negative slope in common liquids. In figure S2, it is observed that the slope is constant in regime I, but decreases fast above $\chi \approx 0.025$ and recovers the negative value in regime III, in agreement with the three different regimes presented in the manuscript and predicted by molecular dynamics simulations.

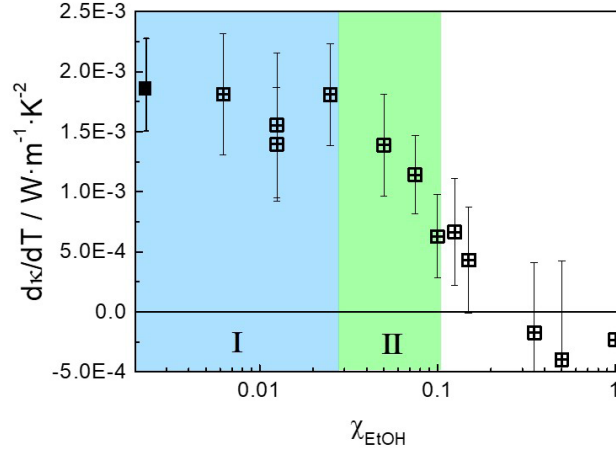


Figure S2. Slope of $\kappa(T)$ for different solutions of EtOH/water, measured from 290 K to the crystallization temperature. The data for pure water (solid square) is in good agreement with the value reported in [3]. The negative value of the temperature dependence coefficient is recovered above ≈ 0.1 , in Region III.

2.- THERMAL CONDUCTIVITY MODELLING

A binary solution model was developed to compare with the experiments. As it is observed in Figure S3, this simple model fits satisfactorily the thermal conductivity curve at concentrations of ethanol larger than $x=0.1$ (Region III).

Thermal transport in liquids depends strongly on the strength and type of interactions between molecules, so that κ of the mixture may be modeled by occurrence of each type of interactions. In this case, there are three different pair interactions possible in a water/ethanol solution: H_2O-H_2O , $H_2O-EtOH$ and $EtOH-EtOH$.

The probability of each of these pair interactions does not depend only on the number, but also on the volume occupied by each molecule. Thus, in a first level of approximation we can consider the average thermal conductivity as the κ of pure components weighted by their volume fraction occupied, ϕ_i :

$$\kappa^2 = \underbrace{\kappa_{H_2O}\phi_{H_2O}\kappa_{H_2O}\phi_{H_2O}}_{\text{water-water}} + \underbrace{\kappa_{H_2O}\phi_{H_2O}\kappa_{EtOH}\phi_{EtOH}}_{\text{water-ethanol}} + \underbrace{\kappa_{EtOH}\phi_{EtOH}\kappa_{EtOH}\phi_{EtOH}}_{\text{ethanol-ethanol}}$$

Considering that $\phi_{H_2O} = 1 - \phi_{EtOH} = 1 - \phi$, the average thermal conductivity can be rewritten as:

$$\kappa = \sqrt{\kappa_{H_2O}^2(1 - \phi)^2 + \kappa_{H_2O}(1 - \phi)\kappa_{EtOH}\phi + \kappa_{EtOH}^2\phi^2} \quad (S1)$$

In Figure S3 we compare the model with experimental thermal conductivity values. Such a simple model reproduces the behavior of the thermal conductivity in a wide concentration range, except in the very diluted regime (Regions I and II identified in the main text).

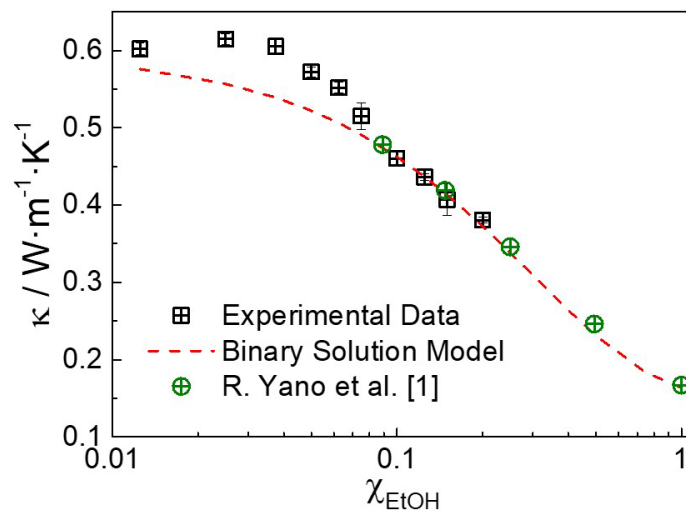


Figure S3. Comparison between the thermal conductivity data measured in this work and the binary solution model (Equation S1) for ethanol. To check the accuracy of the model in the high concentration regime, we also plotted the data by R. Yano et al.⁴ for completeness.

3.- THE BEND + LIBRATION COMBINATION BAND

Previous works showed the sensitivity of the bend + libration combination band to changes in the tetrahedral disposition of water molecules within the H-bond network.⁵ As it is reported in the text, this band helps us to define the different regimes in the solvation of alcohol molecules, which correspond to the different behaviors observed in the thermodynamic properties studied in this work. In Figure S4 we compare the results for the three molecules studied in this work, along with their corresponding thermal conductivities. The results show that the transition between Regime I and II moves to lower concentrations in isopropanol; increasing the length of the alcohol chain makes the definition of the boundary regions less accurate.

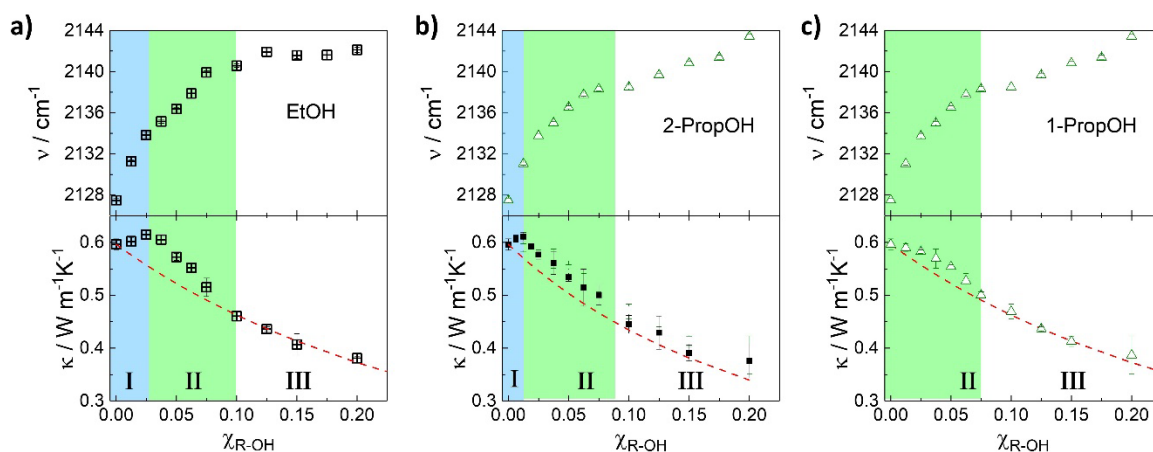


Figure S4. Frequency dependence of the bend + libration combination band with the concentration of the three alcohols studied in this work. The results are compared to their thermal conductivities, for better definition of regions I, II and III.

4.- ISENTROPIC COMPRESSIBILITY

In Figures S5 and S6 we compare the temperature and concentration dependence of the isentropic compressibility for the three alcohols.

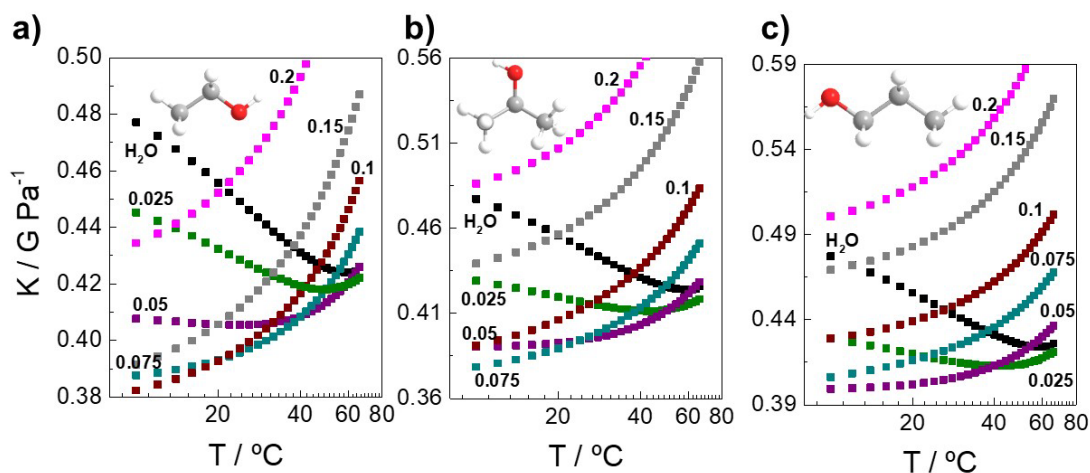


Figure S5. Temperature dependence of the isentropic compressibility for ethanol (a), 2-propanol (b) and 1-propanol (c) for different concentrations of solute.

As it is observed in figure S6a, the rigidity of the system increases at low concentrations of solute, and enhances the speed of sound (Figure S6b). The compressibility increases again (as it is expected due to the disruption of the H-bond network of water) with further increase of the concentration. Consistent with previous measurements, the minimum (maximum in sound velocity) is displaced to lower concentrations as the length of the hydrophobic chain increases.

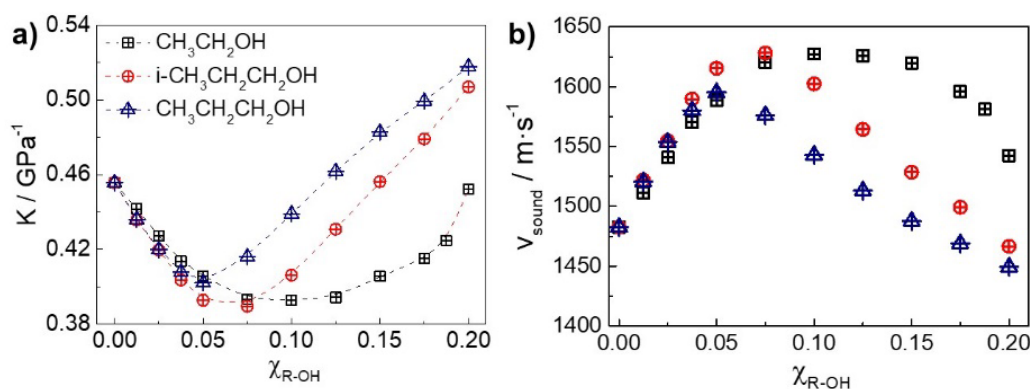


Figure S6. Variation of the isentropic compressibility (a) and sound velocity (b) on the concentration of solute, at $T=20$ °C.

REFERENCES

- (1) Poole, P. H.; Sciortino, F.; Grande, T.; Stanley, H. E.; Angell, C. A. Effect of Hydrogen Bonds on the Thermodynamic Behavior of Liquid Water. *J. Phys. Chem.* **1992**, *96* (12), 7312–7320.
- (2) Ramirez, M. L. V.; Nieto Castro, C. A.; Nagasaka, Y.; Nagashima, A.; Assael, M. J.; Wakeham, W. A. Standard Reference Data for the Thermal Conductivity of Water. *J. Phys. Chem. Ref. Data* **1995**, *24* (3), 1377–1381. <https://doi.org/10.1063/1.555963>.
- (3) Ramirez, M. L. V.; Nieto Castro, C. A.; Nagasaka, Y.; Nagashima, A.; Assael, M. J.; Wakeham, W. A. Standard Reference Data for the Thermal Conductivity of Water. *J. Phys. Chem. Ref. Data* **1995**, *24* (3), 1377–1381. <https://doi.org/10.1063/1.555963>.
- (4) Yano, R.; Fukuda, Y.; Hashi, T. Thermal Conductivity Measurement of Water-Ethanol Solutions by the Laser-Induced Transient Grating Method. *Chem. Phys.* **1988**, *124* (2), 315–319. [https://doi.org/10.1016/0301-0104\(88\)87161-1](https://doi.org/10.1016/0301-0104(88)87161-1).
- (5) Verma, P. K.; Kundu, A.; Poretz, M. S.; Dhooonmoon, C.; Chegwidan, O. S.; Londergan, C. H.; Cho, M. The Bend+Libration Combination Band Is an Intrinsic, Collective, and Strongly Solute-Dependent Reporter on the Hydrogen Bonding Network of Liquid Water. *J. Phys. Chem. B* **2018**, *122* (9), 2587–2599. <https://doi.org/10.1021/acs.jpcc.7b09641>.